ELSEVIER

Thermochimica Acta 273 (1996) 31–42

thermochimica acta

The thermal properties of three (Cl-, Br-, I-) para-halotoluenes. Formation of glassy crystals

J.C. van Miltenburg[a,*], A. Alvarez-Larena[b], M. Labrador[c], L. Palacios[c], J. Rodriguez-Romero[d], E. Tauler[c], E. Estop[b]

[a] *Department of Interfaces and Thermodynamics, Utrecht University, Padualaan 8, 3508 TB Utrecht, The Netherlands*

[b] *Unitat de Cristallografia, Universitat Autonoma de Barcelona, Facultat de Ciencies Cs., 08193 Bellaterra, Spain*

[c] *Departament de Cristallografia, Universitat de Barcelona, Facultat de Geologia, 08028 Barcelona, Spain*

[d] *Institut Quimic de Sarriá, Via Augusta, 390, 08017 Barcelona, Spain*

Received 20 April 1995; accepted 20 June 1995

Abstract

The heat capacities of three para-halotoluenes, *p*-chlorotoluene, *p*-bromotoluene and *p*-iodotoluene, were measured with an adiabatic calorimeter. All three compounds showed the formation of glassy crystals. The glass transition temperatures are 220, 242 and 250 K respectively. The temperature and enthalpies of fusion are: for *p*-chlorotoluene, 280.69 ± 0.01 K and 13554 J mol^{-1}; for *p*-bromotoluene, 299.94 ± 0.01 K and 15127 J mol^{-1}; and for *p*-iodotoluene, 306.70 ± 0.05 K and 14963 J mol^{-1}. The heat capacity of *p*-iodotoluene was measured from 5 K; the derived thermodynamic properties are given. Those of the other compounds were measured from 80 K.

Keywords: Adiabatic calorimetry; Glassy crystal; Halotoluenes

1. Introduction

The syncrystallisation of para-disubstituted benzenes is one of the topics studied in our laboratories. The compounds often form solid solutions and we are interested in

* Corresponding author. Tel.: +31 30532386; Fax: +31 30533946; E-mail: miltenb@chem.ruu.nl.

SSDI 0040-6031(95)02596-0

formulating more detailed conditions for the occurrence of (complete) miscibility in the solid phase. Aspects which attract our special attention are the size of the substituents and the symmetry of the components. Several phase diagrams for binary systems composed of the para-dihalobenzenes (Cl-, Br- and I-) have already been measured [1–4]. Now, we are including a new substituent: the methyl group, thus greatly enlarging the number of possible combinations. Detailed knowledge of the crystallographic and thermodynamic properties of the pure components is of paramount importance. The calculations of the excess properties by the method of the equal Gibbs energy curve [5] (or EGC method) performed on the obtained phase diagrams start with data for the pure components.

In this work we report on the thermodynamic properties of the para-halotoluenes (Cl-, Br-) between 100 K and room temperature. The iodo-compound was measured between 5 and 330 K. To our knowledge, these compounds have not been studied before by adiabatic calorimetry.

2. Experimental

The commercially available products (Fluka) were further purified, the iodo- and bromo-products by sublimation and the chloro-compound by fractional crystallisation. The purity was checked by differential scanning calorimetry and gas chromatography. The purity was estimated to be better than 99.7%.

The adiabatic calorimeter used was described before in detail [6]. The performance of the calorimeter was checked with synthetic sapphire and *n*-heptane and compared to the data published by the National Bureau of Standards. Above 30 K the inaccuracy of the heat capacity data and the other thermodynamic properties which are calculated from these data is within 0.2%, but below 30 K this inaccuracy increases to about 1%. Between 100 and 300 K the imprecision of the calorimeter, as derived from the differences of the experimental data from a fitted curve, is in the order of 0.02%. The thermometer used was calibrated at 16 points between 13 and 300 K (Oxford Instruments Limited) on the IPTS-68 scale; we converted the calibration to ITS-90. The calorimeter was loaded with 7.55, 8.62 and 10.06 g (Cl-, Br- and I-toluene respectively). The vessel was closed under vacuum after admitting about 2000 Pa of helium in order to enhance the heat conduction. The calorimeter vessel and its surrounding shields are mounted under the liquid helium tank in the cryostat. A shield is soft-soldered to the bottom of the cryostat, thus creating a space separated from the high vacuum of the cryostat. This space is evacuated through a by-pass tube which can be closed at the top of the cryostat. Closing this connection and admitting about 100 Pa of helium pressure allows us to cool the vessel and the shields quickly without much evaporation of liquid nitrogen or liquid helium in the tanks. Cooling down from room temperature to 80 K takes about two hours. When the lower tank is filled with liquid helium, cooling from 80 to 4.2 K takes only about half an hour. Before the measurements are started, the vacuum in the space surrounding the vessel is restored. The measurements are completely automated; the operator chooses the end temperature of the measurement, the temperature increment in the successive heat capacity

determinations and some other settings. Measurements are made with a stabilisation period of about 800 s above 100 K and of 400 s between 30 and 100 K. The input period is of the same order. The calculation of the heat capacity data was performed in the usual way by extrapolating the temperature–time curves in the stabilisation periods to the mid-point of the heat input period. This gave us the temperature increment caused by the known amount of heat supplied to the vessel and the heat capacity was calculated. When, however, the product in the vessel is in a metastable state and is relaxing to a more stable state, the temperature–time curves deviate from the normal behaviour expected at that temperature and shield setting. In this case, the heat exchange with the surroundings was taken as a linear function between two temperatures at which the system showed normal behaviour or, if no such equilibrium values could be found, the heat capacities were calculated with the heat exchange found in a previous empty vessel experiment.

3. Results

All three compounds showed two anomalies in the heat capacity curves (see Fig. 1). The high-temperature anomaly is the fusion, the low-temperature a glass transition in the crystalline state. The jump in heat capacity at the glass transition temperature T_g diminishes in the order iodo > chloro > bromo. The curve of *p*-bromotoluene is shifted upwards by 30 J K^{-1} mol^{-1} and for *p*-iodotoluene by 50 J K^{-1} mol^{-1}, for clarity. Table 1 gives the experimental data series. Table 2 gives a polynomial expression for the heat capacities of the glass phase, the crystalline phase between the glass transition and the

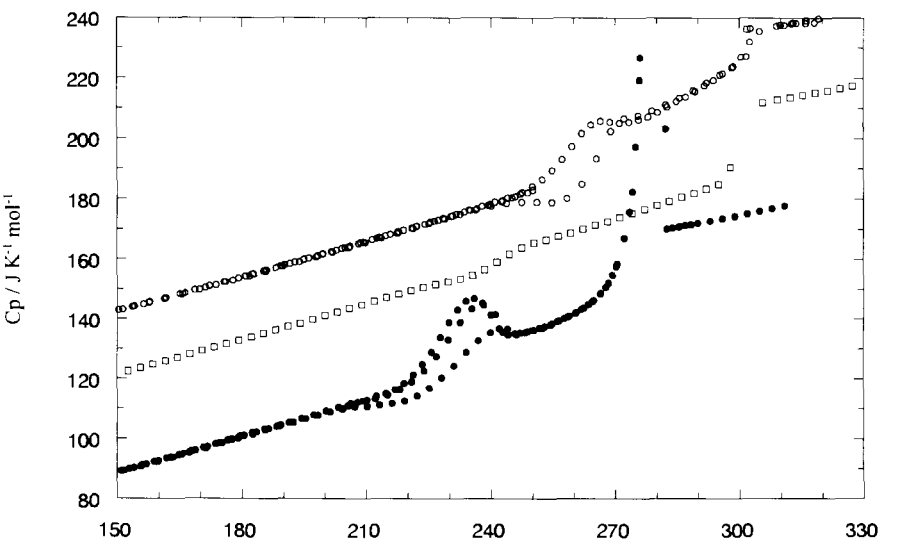

Fig. 1. Heat capacity curves of the three compounds: N, *p*-chlorotoluene; O, *p*-bromotoluene, shifted upwards by 30 J K^{-1} mol^{-1}; and ○, *p*-iodotoluene, shifted upwards by 50 J K^{-1} mol^{-1}.

Table 1
Experimental molar heat capacity data

T/K	C_p/J K^{-1} mol^{-1}	T/K	C_p/J K^{-1} mol^{-1}	T/K	C_p/J K^{-1} mol^{-1}	T/K	C_p/J K^{-1} mol^{-1}	T/K	C_p/J K^{-1} mol^{-1}
p-Chlorotoluene									
Series 1		213.17	112.42	109.32	75.34	241.07	143.13	223.55	126.17
90.18	66.01	216.18	113.03	111.85	74.89	243.98	138.33	225.70	130.31
92.75	67.05	219.19	113.88	114.78	76.01	246.95	137.06	227.82	135.37
95.63	68.24	222.19	115.57	117.71	77.13	249.93	137.98	229.89	140.41
98.50	69.41	225.19	118.20	120.63	78.36	252.90	139.31	231.93	144.66
101.38	70.62	228.17	121.68	123.55	79.48	255.86	140.91	233.95	147.44
104.27	71.75	231.13	125.76	126.48	80.58	258.83	142.81	235.95	148.43
107.16	72.91	234.06	130.23	129.41	81.73	261.79	145.14	237.95	146.94
110.06	74.02	236.97	134.41	132.34	82.86	264.74	148.26	239.97	142.99
112.97	75.19	239.88	137.04	135.28	83.99	267.67	152.87	242.01	138.44
115.88	76.30	242.80	137.25	138.22	85.22	270.58	160.68	244.07	136.36
118.79	77.47	245.75	136.84	141.16	86.39	273.41	178.10	246.14	136.46
121.71	78.59	248.71	137.53	144.10	87.52	276.04	230	248.20	137.14
124.63	79.72	251.67	138.76	147.05	88.68	278.12	445	250.26	138.01
127.56	80.84	254.64	140.23	149.99	89.82	279.34	1257	252.30	138.77
130.48	81.98	257.60	141.99	152.95	90.92	279.87	3126	254.34	139.90
133.42	83.14	260.56	144.09	155.90	92.11	280.12	5901	256.37	141.24
136.35	84.29	263.51	146.84	158.85	93.28	280.26	9709	258.39	142.50
139.29	85.48	266.44	150.79	161.81	94.46	280.35	14791	260.40	143.89
142.23	86.68	269.36	156.94	164.77	95.64	280.41	20788	262.40	145.56
145.17	87.82	272.22	169.35	167.72	96.84	280.45	27063	264.39	147.79
148.11	88.93	274.95	199.87	170.67	98.06	280.49	34065	266.37	150.55
151.05	90.08	277.30	313	173.62	99.27	280.52	42203	268.34	154.01
153.99	91.19	278.88	757	176.58	100.53	280.54	66421	270.30	159.33

156.93	92.37	279.64	1991	179.53	101.84	280.55	63649	272.23	168.71
159.87	93.56	279.99	4094	182.48	103.13	280.57	68675	274.12	184.41
162.81	94.73	280.17	6953	185.44	104.29	281.40	480.70	275.91	222
165.76	95.90	280.29	10837	188.40	105.31	283.79	172.99	277.49	323
168.71	97.10	280.36	15803	191.36	106.48	286.93	173.80	278.70	627
171.66	98.33	280.42	21944	194.32	107.81	289.98	174.54	279.47	1506
174.61	99.56	280.46	28482	197.29	109.06	292.97	175.24	279.92	3563
177.56	100.82	280.49	35910	200.25	110.39	295.96	176.03	280.16	7066
180.51	102.08	280.51	44272	203.21	111.64	298.95	176.83	280.29	11869
183.47	103.27	280.53	46170	206.18	112.97	301.94	177.70	280.38	18030
186.43	104.43	280.55	95558	209.14	113.81	304.93	178.60	280.43	25437
189.38	105.53	280.56	91319	212.12	114.50			280.47	32448
192.34	106.53	280.79	2037	215.09	115.87	Series 3		280.51	42377
195.31	107.73	282.48	172.62	218.06	117.64			280.53	60095
198.27	108.91	285.41	173.39	221.02	120.25	205.50	112.19	280.55	107968
201.24	110.07	288.32	174.08	223.96	124.00	207.81	113.42	280.56	59181
204.21	111.04			226.87	128.88	210.11	114.13	282.18	205.96
207.19	111.84	Series 2		229.75	134.55	212.39	115.41	285.56	173.44
210.17	111.95			232.59	140.39	214.65	116.23	288.41	174.04
p-Bromotoluene									
Series 1		164.44	96.96	220.71	119.48	277.09	146.59	321.38	185.85
112.04	76.88	167.40	98.11	223.67	120.58	280.06	147.89	324.37	186.60
114.53	77.82	170.35	99.30	226.64	121.59	283.04	149.25	327.36	187.48
117.45	78.95	173.31	100.42	229.61	122.51	286.02	150.66	330.35	188.24
120.37	80.09	176.26	101.56	232.59	123.39	289.00	151.92		
123.29	81.24	179.22	102.75	235.57	124.59	291.98	153.32		
126.21	82.37	182.18	103.90	238.54	126.49	294.96	154.87		
129.14	83.48	185.14	105.11	241.50	128.98	297.92	160.58		
132.07	84.59	188.10	106.27	244.46	131.63	299.65	1944		
135.00	85.72	191.06	107.44	247.41	133.77	299.92	120676		

Table 1 (*Continued*)

T/K	C_p/J K^{-1} mol^{-1}	T/K	C_p/J K^{-1} mol^{-1}	T/K	C_p/J K^{-1} mol^{-1}	T/K	C_p/J K^{-1} mol^{-1}	T/K	C_p/J K^{-1} mol^{-1}
137.94	86.84	194.03	108.39	250.36	135.43	299.92	241508		
140.87	87.96	196.99	109.79	253.31	136.42	299.93	440276		
143.81	89.09	199.96	111.07	256.27	137.54	299.93	995211		
146.75	90.20	202.92	112.22	259.24	138.70	299.93	709078		
149.70	91.32	205.89	113.50	262.21	140.03	305.76	181.89		
152.64	92.44	208.86	114.70	265.18	141.35	309.34	182.84		
155.59	93.55	211.83	115.90	268.16	142.50	312.41	183.57		
158.54	94.72	214.79	117.16	271.13	143.89	315.40	184.35		
161.49	95.83	217.75	118.35	274.11	145.24	318.39	185.18		
p-Iodotoluene									
Series 1		243.69	128.80	5.62	1.78	136.48	87.59	284.88	162.33
85.52	67.57	247.36	129.17	7.40	3.45	141.40	89.46	287.13	163.87
90.58	69.70	251.02	129.17	8.84	5.59	146.33	91.30	289.38	165.66
95.44	71.53	254.67	129.09	10.64	7.59	151.29	93.16	291.61	167.60
100.12	73.49	258.31	130.40	12.87	10.29	156.25	94.95	293.82	169.38
104.65	75.34	261.91	135.03	15.18	14.80	161.23	96.71	296.03	171.51
109.05	77.12	265.45	143.52	17.49	18.51	166.20	98.58	298.22	173.59
113.35	78.81	268.90	152.57	20.11	22.40	171.12	100.48	300.40	176.97
117.57	80.51	272.28	156.76	23.00	26.37	175.99	102.40	302.55	182.00
121.70	82.22	275.64	157.74	25.87	29.86	180.80	104.26	304.64	202
125.75	83.69	278.98	159.33	28.47	32.81	185.56	106.18	306.11	752
129.73	85.18	282.30	161.29	30.75	35.08	190.27	108.07	306.60	12403
133.68	86.68	285.60	163.54	32.81	36.82	194.93	109.93	306.65	55429
137.65	88.18	288.88	165.98	34.11	38.61	199.55	111.75	306.67	140710
141.62	89.71	292.13	168.57	36.36	40.14	204.12	113.64	306.67	179639
145.61	91.22	295.36	171.13	39.02	42.29	208.66	115.52	306.68	167125
149.60	92.77	298.56	173.94	42.18	44.61	213.15	117.25	306.69	150586

153.60	94.19	301.74	177.16	45.33	46.75	217.60	119.07	306.70	158132
157.61	95.66	304.87	186	48.53	48.80	222.02	120.88	306.71	239785
161.62	97.25	306.55	4795	51.79	50.84	226.39	122.68	306.71	180355
165.64	98.64	306.69	313615	55.11	52.77	230.74	124.44	306.72	116985
169.66	100.15	306.69	865057	58.49	54.61	235.04	126.17	306.75	34189
173.69	101.66	306.69	$>10^6$	61.92	56.45	239.31	127.92	308.00	299
177.73	103.19	306.69	$>10^6$	65.35	58.17	242.52	129.12	310.80	187.58
181.77	104.73	306.69	$>10^6$	68.69	59.83	244.97	130.45	313.63	188.30
185.81	106.28	306.69	709352	71.86	61.37	247.45	132.19	315.95	188.25
189.86	107.89	306.70	444935	74.92	62.12	249.92	134.13	318.06	188.46
193.89	109.52	306.70	285703	77.87	64.04	252.37	136.49		
197.90	111.09	306.71	193089	80.70	65.32	254.79	139.48		
201.87	112.64	306.71	112612	83.45	66.50	257.20	143.12		
205.81	114.23	307.52	579	86.13	67.63	259.58	147.41		
209.72	115.82	309.87	187.65	88.75	68.73	261.92	151.77		
213.60	117.33	312.94	188.38	93.00	70.28	264.25	154.61		
217.45	118.91	316.01	189.13	97.90	72.63	266.55	155.79		
221.28	120.54	319.08	189.87	102.68	74.56	268.86	155.50		
225.07	122.20	322.13	190.50	107.42	76.43	271.16	155.19		
228.84	123.72	325.18	191.64	112.19	78.34	273.47	155.51		
232.59	125.21	328.22	192.19	116.99	80.18	275.76	156.30		
236.31	126.60	331.25	186.56	121.83	82.09	278.06	157.17		
240.01	127.85	Series 2		126.69	83.87	280.34	158.70		

Table 2
Linear fit coefficients $C_p = a_0 + a_1 T$ of the heat capacities and the corresponding temperature range

	Coefficients		Temperature range	
	a_0/J K^{-1} mol^{-1}	a_1/J K^{-2} mol^{-1}	T_1/K	T_2/K
p-Chlorotoluene				
Glassy crystal	29.99	0.3924	160	200
Crystalline phase	12.75	0.5012	245	255
Liquid phase	98.62	0.2618	283	310
p-Bromotoluene				
Glassy crystal	30.99	0.4005	160	225
Crystalline phase	21.71	0.4506	250	290
Liquid phase	103.27	0.257	300	330
p-Iodotoluene				
Glassy crystal	33.17	0.3925	160	225
Crystalline phase	−55.7	0.765	280	300
Liquid phase	105.27	0.265	305	325

Table 3
The enthalpies of melting and the melting temperatures, the estimated glass transition temperatures and the associated heat capacity jump

Compound	T_{fus}/K	$\Delta_{fus}H$/J mol^{-1}	T_g/K	$\Delta C_p(T_g)$/J K^{-1} mol^{-1}
p-Chlorotoluene	280.69 ± 0.01	13554 ± 3	220	7.8[a]
p-Bromotoluene	299.94 ± 0.01	15127	242	4.5
p-Iodotoluene	306.70 ± 0.05	149.63 ± 6	250	12.4[a]

[a] Less reliable due to pre-melting.

melting point, and the liquid phase. In Table 3 the melting points and the enthalpy of fusion are given and also the estimates of the glass transition temperatures and the corresponding heat capacity jumps. We could not find a clear relation between the enthalpy of fusion and the molar mass. Table 4 lists the derived thermodynamic properties for *p*-iodotoluene which were measured from 5 to 330 K.

3.1. *Fusion and purity determination*

The temperature of fusion and the purity of the sample were calculated from the interrupted melting experiments. After each energy addition, the sample was stabilised and the equilibrium temperature determined. The data were plotted as $1/F$ against T in which F is the fraction melted at the temperature T. Using the van't Hoff relation for the freezing point depression, the purity can be calculated if the impurity forms a eutectic phase diagram with the main component. The plots are given in Fig. 2 and

Table 4
Thermodynamic properties at selected temperatures for *p*-iodotoluene ($M = 0.218037\,kg\,mol^{-1}$)

T/K	C_p/J mol^{-1} K^{-1}	$S^0(T)-S^0(0)$/ J mol^{-1} K^{-1}	$H^0(T)-H^0(0)$/ J mol^{-1}	$-[G^0(T)-H^0(0)]/T$ J mol^{-1} K^{-1}
10	6.915	2.666	18.96	0.7700
20	22.25	11.93	161.93	3.834
30	34.04	23.35	447.48	8.431
40	43.03	34.45	835.81	13.56
50	49.72	44.80	1301	18.79
60	55.43	54.38	1827	23.93
70	60.48	63.31	2407	28.93
80	65.01	71.66	3033	33.75
90	69.21	79.57	3704	38.41
100	73.49	87.07	4417	42.90
110	77.46	94.26	5172	47.25
120	81.37	101.17	5966	51.45
130	85.16	107.83	6799	55.54
140	88.93	114.28	7669	59.50
150	92.68	120.54	8577	63.36
160	96.27	126.64	9522	67.13
170	100.04	132.59	10503	70.81
180	103.94	138.42	11523	74.40
190	107.97	144.15	12583	77.92
200	111.94	149.79	13682	81.37
210	116.05	155.35	14822	84.76
220	120.05	160.84	16003	88.10
230	124.15	166.26	17224	91.38
240	128.19	171.63	18485	94.61
250	134.20	176.97	19793	97.80
260	148.19	182.47	21195	100.95
270	155.35	188.28	22735	104.07
280	158.43	193.96	24297	107.18
290*	166.15	199.65	25920	110.27
300*	173.80	205.42	27620	113.35
306.70^{s}*	178.93	209.31	28802	115.40
306.70^{l}*	186.50	258.10	43764	115.40
310	187.42	260.10	44381	116.93
320	190.07	266.09	46269	121.50
330	192.73	271.98	48183	125.97

Key: *, extrapolated; ^{s}, solid; ^{l}, liquid.

from them it is clear that the purity cannot be calculated by this method for *p*-iodotoluene. However, because the melting process for this compound takes place in a very narrow temperature range (in the order of 0.04 K), we assume that the compound is very pure. For *p*-chlorotoluene, we found a purity of 99.73% and for *p*-bromotoluene, 99.994%. Since the latter value is exceptionally high, we think that purification by sublimation works very well for this compound as large and beautiful crystals are rapidly formed.

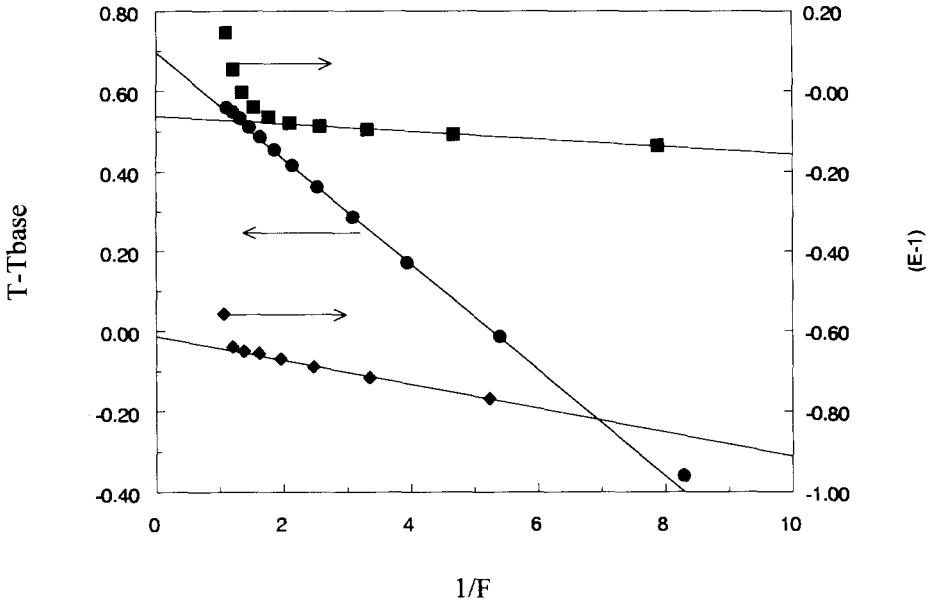

Fig. 2. The three melting experiments. The equilibrium temperatures in the melt are plotted against the reciprocal of the melted fraction: ●, *p*-chlorotoluene, temperature axis minus 280 K, plotted on the left *y*-axis; ◆, *p*-bromotoluene, plotted on the right axis, minus 300 K; and ■, *p*-iodotoluene, plotted on the right axis minus 306.7 K.

The enthalpy of fusion was calculated in an iterative way. The linear fits of the heat capacity before and after the fusion are taken as a first baseline and extrapolated to the temperature of highest value in the heat capacity. Then the enthalpy of fusion is calculated and the baseline is adjusted to the melted fraction. This process gives a sigmoidal baseline; repeating the calculation three or four times results in a stable value for the enthalpy of fusion. Repeated melting experiments with the same charge in the calorimeter results in a very small standard deviation in the enthalpy of fusion, at maximum 0.005%. This reflects, however, the precision of the calorimeter and the inaccuracy of 0.2% mentioned before also applies to these values.

3.2. The glass transition

In Fig. 3 the rate of temperature drift in the stabilisation periods multiplied by the heat capacity is plotted against the temperature in the region of the glass transition of *p*-chlorotoluene. The molar heat capacities measured in those runs are also given. The normal drift of the calorimeter in this region caused by the inevitable deviation from complete adiabatic behaviour is about 40 μW. Approaching the glass transition temperature from low temperature, the sample exhibits first an exothermic effect, corresponding to the relaxation of the glass. After the glass transition, the compound is in a state in which the enthalpy is lower than the equilibrium value, and the drift

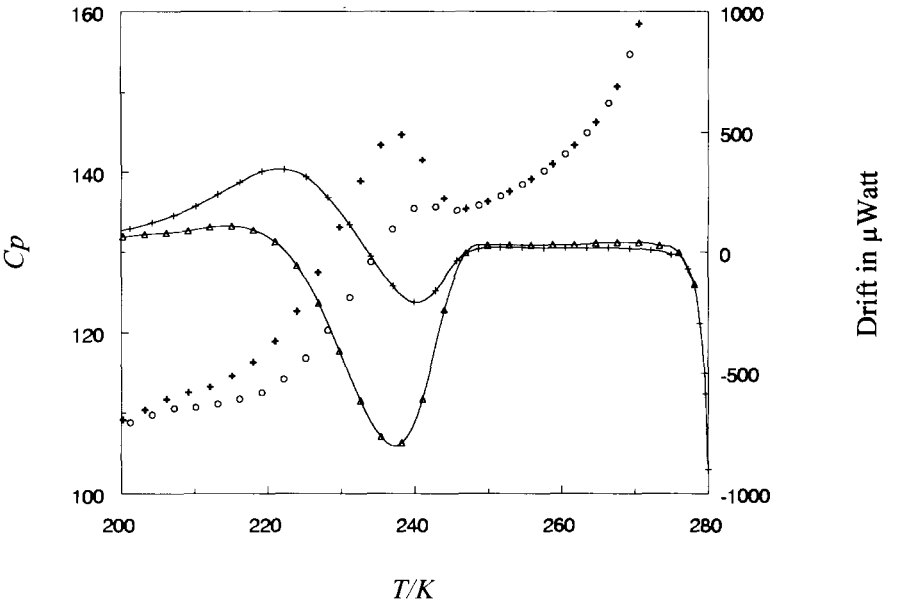

Fig. 3. The glass transition in *p*-chlorotoluene: +, without prior stabilisation; △ after stabilisation at 220 K. The drawn curves, representing the drift, are plotted on the right axis.

becomes endothermic. The summation of these two effects is roughly equal to zero, thus indicating that the enthalpy loss before the glass transition is recovered after the transition. We did an experiment in which we relaxed the glass for over two days close to the temperature where the exothermic effect was maximal; then we recooled the vessel and repeated the heat capacity measurements passing through the glass transition. The exothermic effect had almost completely disappeared and the endothermic effect became larger as a result of this thermal treatment. This confirms the already known fact that a glass relaxes to a lower enthalpy state, without, however, reaching thermodynamic equilibrium within the experimental time. The temperature–time curve of the relaxation process close to the glass transition is of an exponential form, with the natural drift of the calorimeter added as a linear function. Fitting these data to the model proposed by Williams and Watts [7]

$$\Delta T(t) = \Delta T(0) \exp(-(t/\tau)^{\beta})$$

as done by Fujimori and Oguni [8] for the glass transition in 2-bromothiophene, gave a value of 0.765 for β and 22735 s for τ with a standard deviation of 7×10^{-4} K. This standard deviation is quite high and the reliability of the value for β may be questioned. The same experiment was done for *p*-iodotoluene and the experimental data are given in Table 1. The glass transition in *p*-bromotoluene was measured only once. The molar heat capacities of the relaxed glass and the glass formed by rapid cooling are indistinguishable within the precision of the calorimeter.

4. Discussion

The thermal properties of three *p*-halotoluenes were measured. All three compounds show the formation of glassy crystals. For a discussion of this not so well-known phase, we refer to a recent article by Suga [9]. We did not manage to avoid this transition by forming a new stable crystal phase, which one might expect to realize at lower temperatures. It is interesting to point out that the formation of glassy crystals was not observed in the para-halobenzenes [4]. The introduction of the methyl-group gives additional degrees of freedom to the molecules in the crystal. We strongly suspect that the glass transition is caused by the freezing of these degrees of freedom. A structural study clarifying the nature of the disorder in the three halotoluenes is under way.

The melting enthalpies and melting temperatures are given. No obvious relation to the molar mass was found. The entropy increments for *p*-iodotoluene are given from 0 K and these values might be used when the entropy values are calculated from spectroscopic data to find the residual entropy of the glass.

References

[1] Y. Haget, J.R. Housty, A. Maiga, L. Bonpunt, N.B. Chanh, M.A. Cuevas and E. Estop, J. Chim. Phys., 81 (1984) 197–206.
[2] M. Labrador, T. Calvet, E. Tauler, X. Alcobé, M.A. Cuevas, E. Estop and Y. Haget, J. Chim. Phys., 84 (1987) 951–955.
[3] T. Calvet, Doctoral Thesis, University of Barcalona, 1990.
[4] P.J. van der Linde, Doctoral Thesis, Utrecht University, 1992.
[5] H.A.J. Oonk, Phase Theory, The Thermodynamics of Heterogenous Equilibria, Elsevier Science, Amsterdam, 1981.
[6] J.C. van Miltenburg, G.J.K. van den Berg and M.J. van Bommel, J. Chem. Thermodyn., 19 (1987) 1129–1137.
[7] G. Williams and D.C. Watts, Trans. Faraday Soc., 66 (1970) 80.
[8] H. Fujimori and M. Oguni, J. Phys. Chem. Solids, 54 (1993) 271–280.
[9] H. Suga, Thermochim. Acta, 245 (1994) 69.